Inorganic Chemistry

Article

pubs.acs.org/IC

# Functional Metal–Organic Frameworks via Ligand Doping: Influences of Ligand Charge and Steric Demand

Cheng Wang,[†,‡] Demin Liu,[†] Zhigang Xie,[‡] and Wenbin Lin*[,†]

[†]Department of Chemistry, University of Chicago, 929 East 57th Street, Chicago, Illinois 60637, United States

[‡]Department of Chemistry, CB#3290, University of North Carolina, Chapel Hill, North Carolina 27599, United States

Supporting Information

**ABSTRACT:** Doping a functional ligand into a known crystalline system built from ligands of similar shape and length provides a powerful strategy to construct functional metal–organic frameworks (MOFs) with desired functionality and structural topology. This mix-and-match approach mimics the widely applied metal ion doping (or solid solution formation) in traditional inorganic materials, such as metal oxides, wherein maintaining charge balance of the doped lattice and ensuring size match between doped metal ions and the parent lattice are key to successful doping. In this work, we prepared three sterically demanding dicarboxylate ligands based on Ir/Ru-phosphors with similar structures and variable charges (−2 to 0), $[Ir(ppy)_3]$-dicarboxylate ($\mathbf{L_1}$, ppy is 2-phenylpyridine), $[Ir(bpy)(ppy)_2]^+$-dicarboxylate ($\mathbf{L_2}$, bpy is 2,2′-bipyridine), and $Ru(bpy)_3]^{2+}$-dicarboxylate ($\mathbf{L_3}$), and successfully doped them into the known IRMOF-9/-10 structures by taking advantage of matching length between 4,4′-biphenyl dicarboxylate (BPDC) and $\mathbf{L_1}$–$\mathbf{L_3}$. We systematically investigated the effects of size and charge of the doping ligand on the MOF structures and the ligand doping levels in these MOFs. $\mathbf{L_1}$ carries a −2 charge to satisfy the charge requirement of the parent $Zn_4O(BPDC)_3$ framework and can be mixed into the IRMOF-9/-10 structure in the whole range of $H_2\mathbf{L_1}$/$H_2$BPDC ratios from 0 to 1. The steric bulk of $\mathbf{L_1}$ induces a phase transition from the interpenetrated IRMOF-9 structure to the non-interpenetrated IRMOF-10 counterpart. $\mathbf{L_2}$ and $\mathbf{L_3}$ do not match the dinegative charge of BPDC in order to maintain the charge balance for a neutral IRMOF-9/-10 framework and can only be doped into the IRMOF-9 structure to a certain degree. $\mathbf{L_2}$ and $\mathbf{L_3}$ form a charge-balanced new phase with a neutral framework structure at higher doping levels (>8% For $\mathbf{L_2}$ and >6% For $\mathbf{L_3}$). This systematic investigation reveals the influences of steric demand and charge balance on ligand doping in MOFs, a phenomenon that has been well-established in metal ion doping in traditional inorganic materials.

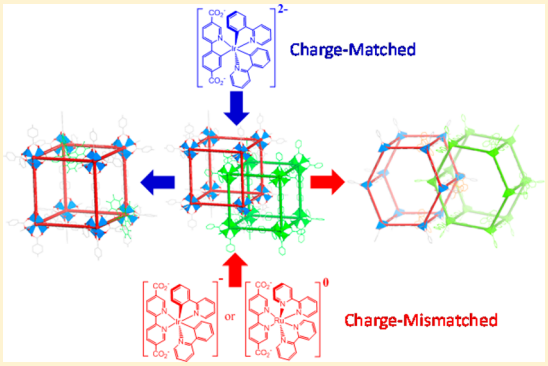


## INTRODUCTION

Metal–organic frameworks (MOFs) have recently emerged as a new class of functional materials whose properties can be readily tuned at the molecular level.[1−5] Rational design and incorporation of building blocks with various functionalities into MOF structures permit the synthesis of a variety of MOFs for applications in many areas, including gas storage,[6−8] chemical sensing,[9−12] catalysis,[13−17] biomedical imaging,[18−20] and drug delivery.[21−23]

The art of systematic structure engineering and property tuning is best illustrated by isoreticular MOFs (IRMOFs) that are constructed by linking metal-coordinated secondary building units (SBUs) with bridging ligands of varied length or functional groups.[6,10,24−33] IRMOFs adopt the same framework topology but possess tunable pore sizes and properties. However, it is not always possible to assemble a functional ligand into a predesigned framework structure, particularly when substantial steric demands are imposed by the functional entities. Postsynthetic modifications (PSM) of interior MOF channels have been utilized to successfully introduce functional groups that cannot be directly incorporated.[34−36] However, PSM tends to reduce the open channel sizes, thus adversely affecting material properties in many cases. Here we propose an attractive alternative to constructing materials possessing desired functionality and crystal structures by doping a fraction of functional ligand into a known crystalline phase built from a much simpler ligand of identical length.[37−46] This mix-and-match approach mimics the widely adopted metal ion doping strategy in traditional inorganic materials (e.g., metal oxides) to not only allow the incorporation of sterically demanding functional ligands into the parent framework but also retain the porosity of the framework for various applications. The ligand doping strategy reported in this paper is distinct from the widely reported metal ion doping into a host MOF structure.[47−51]

In conventional doped metal oxides (or solid solutions), the two most significant parameters dictating the degree of doping are (a) the size match between doped metal ions and the parent lattice and (b) the maintenance of charge balance of the doped

**Received:** August 5, 2013
**Published:** January 14, 2014

   dx.doi.org/10.1021/ic402015q | *Inorg. Chem.* 2014, 53, 1331−1338

**Scheme 1**

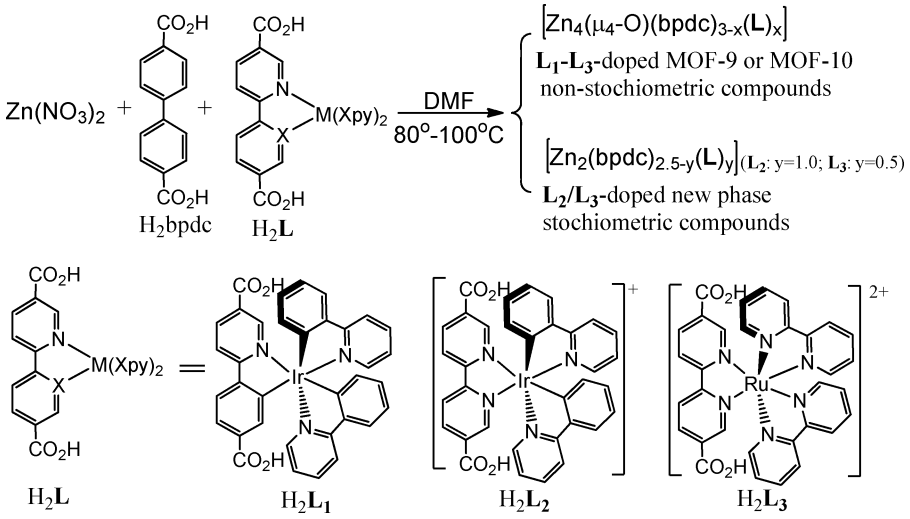


lattice.[52,53] In our proposed mix-and-match strategy for MOF synthesis, it is interesting to test if the size and charge of the doping ligand are also determining factors for the doping level in a certain structure. In this work, we prepared three sterically demanding dicarboxylate ligands based on Ir/Ru-phosphors with similar structures and variable charges (−2 to 0), $[Ir(ppy)_3]$-dicarboxylate ($\mathbf{L_1}$, ppy is 2-phenylpyridine), $[Ir(bpy)(ppy)_2]^+$-dicarboxylate ($\mathbf{L_2}$, bpy is 2,2′-bipyridine), and $Ru(bpy)_3]^{2+}$-dicarboxylate ($\mathbf{L_3}$), and successfully doped them into known IRMOF-9/-10 structures, in the hope of systematically investigating the aforementioned questions in MOF doping.

The Ir-based cyclometalated complexes $[Ir(ppy)_3]$ and $[Ir(bpy)(ppy)_2]^+$ and the Ru complex $[Ru(bpy)_3]^{2+}$ are highly efficient phosphors with long-lived $^3$MLCT excited states.[54−56] Extensive research efforts have been devoted to developing light-emitting devices based on these molecules.[57−59] The $^3$MLCT phosphorescence can also be quenched through energy transfer to molecules with a triplet ground state such as oxygen[11] or via a redox process between the $^3$MLCT state and a quencher.[60] These phosphorescent Ir- and Ru-based molecules are thus suitable for applications in chemical sensing through energy transfer[61] and in photocatalysis via redox quenching.[62−64]

IRMOF-9/-10 structures were chosen to host the Ir/Ru phosphor ligands. IRMOF-9/-10 are a pair of catenation isomers constructed from the biphenyldicarboxylic acid (BPDC) ligand and $[Zn_4(\mu_4\text{-}O)(O_2CR)_6]$ SBUs, forming three-dimensional (3D) structures of the primitive cubic network (pcu) topology. IRMOF-9 has a 2-fold interpenetrated structure, while IRMOF-10 is the non-interpenetrated counterpart. Ligands $\mathbf{L_1}$−$\mathbf{L_3}$ possess matching length to BPDC to allow their doping into IRMOF-9/-10 structures. As $\mathbf{L_1}$ carries a −2 charge to satisfy the charge requirement of the parent $Zn_4O(BPDC)_3$ framework, it can be mixed into the IRMOF-9/-10 structures in the whole range of $H_2\mathbf{L_1}$/$H_2$BPDC ratios from 0 to 1. With increasing doping levels of $\mathbf{L_1}$, the crystals change from the interpenetrated IRMOF-9 structure to the non-interpenetrated IRMOF-10 structure due to the steric demand of the $\mathbf{L_1}$ ligand. The $\mathbf{L_2}$ and $\mathbf{L_3}$ ligands, on the other hand, can only be doped into IRMOF-9/-10 structures to a certain degree before a charge-balanced new phase with neutral framework appears at higher doping levels. Our work illustrates a delicate balance between steric demand and charge balance for ligand doping in MOFs.

## EXPERIMENTAL SECTION

**General Information.** All starting materials were purchased from Aldrich and Fisher, unless otherwise noted, and used without further purification. $^1$H NMR spectra were recorded on a Bruker NMR 400 DRX spectrometer at 400 MHz and referenced to the proton resonance resulting from incomplete deuteration of deuterated chloroform ($\delta$ 7.26). $^{13}$C{$^1$H} NMR spectra were recorded at 100 MHz, and all of the chemical shifts are reported downfield in ppm relative to the carbon resonance of chloroform-$d_1$ ($\delta$ 77.0). Mass spectrometric analyses were conducted using positive-ion electrospray ionization on a Bruker BioTOF mass spectrometer. Single crystal and powder X-ray diffraction analyses were carried out on a Bruker SMART APEX II diffractometer system equipped with Cu-target X-ray tube and operated at 1600 W. For single crystal diffraction, the frames were integrated with Bruker SAINT built into the APEX II software package using a narrow-frame integration algorithm, which also corrects for the Lorentz and polarization effects. Absorption corrections were applied using SADABS for all of the crystals. The PXRD patterns were processed with the APEX II package using PILOT plug-in. UV−vis absorption spectra were obtained using a Shimadzu UV-2401 PC UV−vis Recording spectrophotometer. Thermogravimetric analysis (TGA) was performed using a Shimadzu TGA-50 equipped with a platinum pan, and all samples were heated at a rate of 5 °C/min under air. Nitrogen adsorption experiments were performed with a Quantachrome Autosorb-1C.

**General Synthesis and Characterization of L/BPDC Mixed Zn-MOF Series.** Mixtures of $H_2\mathbf{L}$ and $H_2$BPDC with varying molar ratios were reacted with $Zn(NO_3)_2{\cdot}6H_2O$ in *N*,*N*′-dimethylformamide (DMF) under solvothermal conditions. The molar ratio of $Zn(NO_3)_2$: ($H_2\mathbf{L}$ + $H_2$bpdc): DMF was 0.5−3: 1: 2000. The resulting mixtures were placed in an oven at 100 °C for 1−2 days. Yellow-red crystals with thin plate or feather-like morphologies (depending on resulting phases) were obtained after filtration. Phases of the obtained MOFs were determined by PXRD. Phases of the interpenetrated IRMOF-9 and the non-interpenetrated IRMOF-10 can be differentiated by examining the crystals under polarized light. IRMOF-9, crystallizing in orthorhombic crystal system, exhibited anisotropic birefringent behavior under polarized light, while IRMOF-10, crystallizing in cubic crystal system, was optically isotropic. Thermogravimetric analysis (TGA) measuring the solvent weight loss was used to support the above identification of interpenetrated vs non-interpenetrated phases. The Ir/Ru-complex ($\mathbf{L_1}$ to $\mathbf{L_3}$) contents in all of the MOFs were determined by dissolving a known amount of MOFs in 3 mL of a basic water/ethanol mixture and taking UV−vis measure-


dx.doi.org/10.1021/ic402015q | Inorg. Chem. 2014, 53, 1331−1338

ments of the solution at 375.5 nm. The **L** contents per mass could be determined from standard curves, and the molar doping levels [mol **L**/(mol bpdc + mol **L**)] were then calculated, based on framework formulas of different phases. Whenever mixed phases were encountered, estimations based on an average formula were adopted. Framework formulas of the stochiometric phases **MOF-1** to **MOF-3** were deduced from X-ray crystal structures and the doping level was determined from UV−vis measurements, while the solvent contents were established from a combination of $^1$H NMR and TGA studies.

## RESULTS

**Ligand Synthesis.** The Ir complexes $H_2\mathbf{L}_1$ and $H_2\mathbf{L}_2$ were synthesized by reacting $[Ir(ppy)_2Cl_2]_2$ with methyl-6-(4-(methoxycarbonyl)phenyl)nicotinate [5,5′-$(MeO_2C)_2$-ppy] or diethyl(2,2′-bipyridine)-5,5′-dicarboxylate [5,5′-$(EtO_2C)_2$-bpy], followed by base-promoted hydrolysis (Supporting Information). The Ru-complex $H_2\mathbf{L}_3$ was synthesized following the published procedure by directly reacting cis-$[Ru(bpy)_2Cl_2]$ with 2,2′-bipyridine 5,5′-dicarboxylic acid [5,5′-$(HO_2C)_2$-bpy] (Supporting Information). Syntheses and characterization of these ligands were reported previously.[43,46,65]

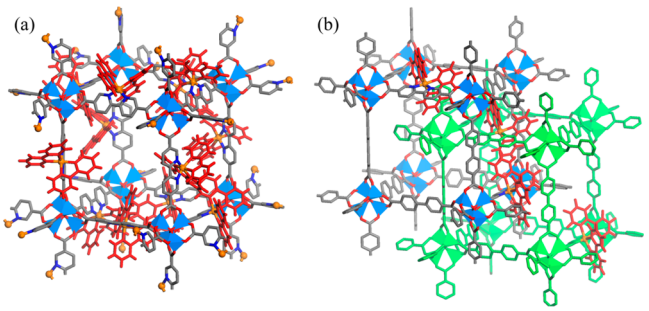


**Figure 1.** (a) Stick/polyhedral model for $\mathbf{L}_1$-doped non-interpenetrated IRMOF-10 structure. (b) Stick/polyhedral model for $\mathbf{L}_1$-doped interpenetrated IRMOF-9 structure.

**Systematic Doping Studies of $\mathbf{L}_1$-Based MOFs.** We hypothesized that Ir/Ru phosphor-based dicarboxylate ligands $\mathbf{L}_1$−$\mathbf{L}_3$ can link the octahedral $[Zn_4(\mu_4\text{-}O)(O_2CR)_6]$ SBUs to form isoreticular MOFs (IRMOF-9 or IRMOF-10 structure) of the pcu topology. Reactions between $H_2\mathbf{L}_1$ and $Zn(NO_3)_2\cdot 6H_2O$ in DMF afforded red single crystals of $[Zn_4(\mu_4\text{-}O)(\mathbf{L}_1)_3]\cdot 64DMF\cdot 35H_2O$ (MOF-**1**). MOF-**1** crystallizes in the cubic $Fm\bar{3}m$ space group with 1/8 of $\mathbf{L}_1$ ligands and 1/24 of $Zn_4(\mu_4\text{-}O)$ clusters which are composed of one Zn atom of 1/6 occupancy and one O atom of 1/24 occupancy in the asymmetric unit. As expected, the carboxylate groups from six adjacent $\mathbf{L}_1$ ligands coordinate to the four Zn centers to form $[Zn_4(\mu_4\text{-}O)(carboxylate)_6]$ SBUs which link $\mathbf{L}_1$ ligands to form a non-interpenetrated 3D network of the IRMOF-10 structure (Figure 1a). $\mathbf{L}_1$ ligands were disordered over two positions as a result of the rotation of the C−C bond between the carboxylate groups and the aromatic rings, a common phenomenon observed when 2-connected dicarboxylate acids were employed as linkers. PLATON calculations indicated that **1** possesses 79% void space that is filled by DMF or water molecules. The disordered nature of the solvent molecules precluded their precise location by X-ray crystallography. The solvent contents were instead established by a combination of $^1$H NMR studies and thermogravimetric analyses (Supporting Information).

In contrast to the formation of the non-interpenetrated IRMOF-10 structure from reactions between $H_2\mathbf{L}_1$ and $Zn(NO_3)_2\cdot 6H_2O$ in DMF, reactions between $H_2$BPDC and $Zn(NO_3)_2\cdot 6H_2O$ under similar reaction conditions in DMF yielded interpenetrated IRMOF-9.[6] Given the similar length of these two dicarboxylate ligands, the formation of MOF-**1** of the non-interpenetrated IRMOF-10 structure can be attributed to the steric bulk of the $\mathbf{L}_1$ ligand. When a mixture of $H_2\mathbf{L}_1$ and $H_2$BPDC in varying molar ratios was reacted with $Zn(NO_3)_2\cdot 6H_2O$ in DMF under solvothermal conditions, crystalline samples were obtained from all of the reaction vials. On the basis of PXRD patterns (Figure 2a), $\mathbf{L}_1$ forms a solid solution with BPDC to adopt IRMOF-9/-10 structures in the whole range of $L_1$/BPDC molar ratios from 0 to 1 (Table 2). Here "solid solution" refers to MOF crystals that are built from a mixture of two ligands of similar shape and length in the same structure. The two ligands occupy the same crystallographic position statistically. It is necessary to differentiate between the formation of a "solid solution" and a mixture of two crystals constructed from two different ligands. In this case, as the $\mathbf{L}_1$ ligand is red and the bpdc ligand is colorless, any crystals that are colored must contain $\mathbf{L}_1$ ligand. In the experiment, even with a very small amount of $\mathbf{L}_1$ ligand added in the synthesis, every crystal under the microscope appeared to be colored (see Figure S3, Supporting Information for a photo of sample $\mathbf{L}_1$-BPDC-2). The light orange color indicates that those crystals cannot be 100% of $\mathbf{L}_1$ ligand either. We thus believe that $\mathbf{L}_1$ ligand and bpdc ligand can form solid solutions.[37−46] We cannot, however, rule out the possible variations of the $\mathbf{L}_1$/bpdc ratios in different crystals. Although PXRD patterns of IRMOF-9 and IRMOF-10 are very similar, these two phases can be differentiated by examining the crystals under polarized light. IRMOF-9, crystallizing in the orthorhombic crystal system (space group $C222_1$), exhibits anisotropic birefringent behavior under polarized light. On other hand, IRMOF-10 crystallizes in the cubic crystal system (space group $Fm\bar{3}m$) and is optically isotropic. The crystals change from the interpenetrated IRMOF-9 structure to the non-interpenetrated IRMOF-10

**Table 1. Key Crystallographic Data for MOFs 1−3**

| | MOF-1 | MOF-2 | MOF-3 |
|---|---|---|---|
| framework formula | $[Zn_4O(\mathbf{L}_1)_3]$ | $[Zn_2(BPDC)_{1.5}(\mathbf{L}_2)]$ | $[Zn_2(BPDC)_2(\mathbf{L}_3)_{0.5}]$ |
| space group | $Fm\bar{3}m$ | $C222_1$ | $C222_1$ |
| cell dimensions (Å) | 34.0 × 34.0 × 34.0 | 18.4 × 26.3 × 42.4 | 18.5 × 26.9 × 41.8 |
| interpenetration | none | 2-fold | 2-fold |
| void space % calcd by PLATON | 79 | 45 | 60 |
| solvent content[a] | $64DMF\cdot 35H_2O$ | $2DMF\cdot 7H_2O$ | $9DMF\cdot 8H_2O$ |
| solvent weight loss (%) | 68 | 19 | 47 |
| calculated framework density (g/cm$^3$) | 0.843 | 0.800 | 0.601 |

[a]Solvent contents were determined by a combination of $^1$H NMR spectroscopy and TGA. See Supporting Information for detailed analyses.


dx.doi.org/10.1021/ic402015q | Inorg. Chem. 2014, 53, 1331−1338

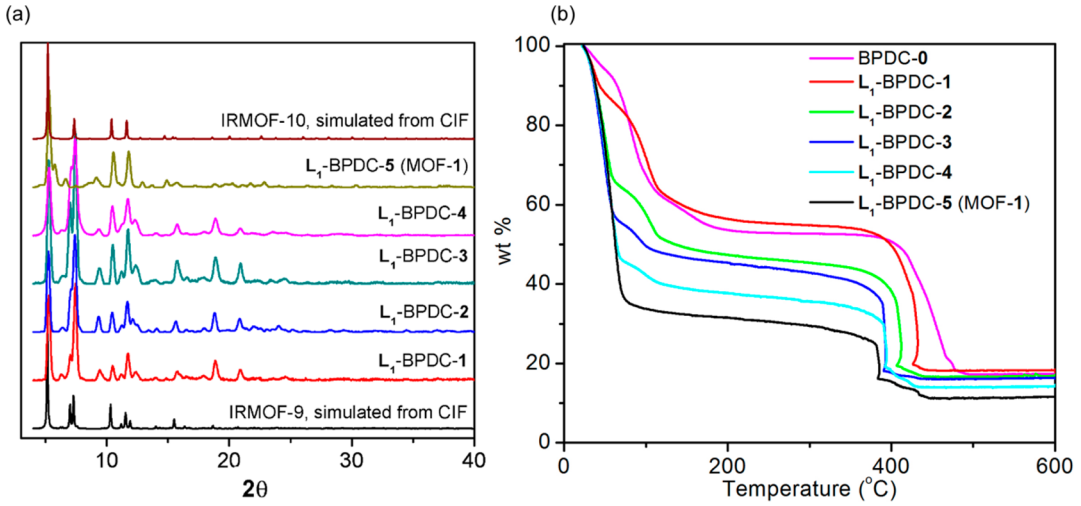


**Figure 2.** (a) PXRD patterns for $L_1$-doped IRMOF-9/-10 samples; (b) TGA of $L_1$-doped IRMOF-9/-10 samples. Preparation conditions, BPDC/$L_1$ content ratios, and the identified phases of all of the samples in (a) and (b) are listed in Table 2. The samples from $L_1$-BPDC-**1** to $L_1$-BPDC-**5** change from the IRMOF-9 structure to the IRMOF-10 structure.

**Table 2. L Ligand Doping Levels Determined by UV-Vis Spectroscopy**

| ligand and sample number | molar ratio of $Zn(NO_3)_2/H_2L/H_2$bpdc in the synthesis | phases determined from PXRD/optical observation/TGA | doping level L/(L + BPDC) (%) |
|---|---|---|---|
| BPDC-**0** | 2/0/1 | IRMOF-9 | 0 |
| $L_1$-BPDC-**1** | 26/1/12 | IRMOF-9 | 4.5 |
| $L_1$-BPDC-**2** | 8/1/3 | IRMOF-9 + IRMOF-10[a] | 17 |
| $L_1$-BPDC-**3** | 4/1/1 | IRMOF-9 + IRMOF-10 | 39 |
| $L_1$-BPDC-**4** | 8/3/1 | IRMOF-9 + IRMOF-10 | 61 |
| $L_1$-BPDC-**5** | 6/1/0 | IRMOF-10 (MOF-**1**) | 100 |
| $L_2$-BPDC-**1** | 26/1/13 | IRMOF-9 | 6 |
| $L_2$-BPDC-**2** | 20/1/9 | IRMOF-9 | 8 |
| $L_2$-BPDC-**3** | 14/1/6 | IRMOF-9 + MOF-**2**[b] | 14 |
| $L_2$-BPDC-**4** | 8/1/3 | IRMOF-9 + MOF-**2** | 26 |
| $L_2$-BPDC-**5** | 4/1/1 | IRMOF-9 + MOF-**2** | 32 |
| $L_2$-BPDC-**6** | 8/3/1 | MOF-**2** | 40 ± 5 |
| $L_2$-BPDC-**7** | 12/5/1 | MOF-**2** | 40 ± 5 |
| $L_2$-BPDC-**8** | 20/9/1 | MOF-**2** | 42 ± 5 |
| $L_2$-BPDC-**9** | 4/1/0 | unknown phase | 100 |
| $L_3$-BPDC-**1** | 6.5/4.4/1 | IRMOF-9 | n.a. |
| $L_3$-BPDC-**2** | 6.6/3/1 | IRMOF-9 | 3.8 |
| $L_3$-BPDC-**3** | 5.9/1/1 | IRMOF-9 | 6 |
| $L_3$-BPDC-**4** | 17.7/1/12 | IRMOF-9 + MOF-**3**[b] | 16.5 |
| $L_3$-BPDC-**5** | 17.7/1/18 | IRMOF-9 + MOF-**3** | 17 |
| $L_3$-BPDC-**6** | 17.7/1/22 | MOF-**3** | 21 ± 3 |
| $L_3$-BPDC-**7** | 17.7/1/33 | MOF-**3** | 22 ± 3 |

[a]This is a mixture of IRMOF-9 and IRMOF-10 phases, based on optical observation and TGA. [b]These are mixture of IRMOF-9 and MOF-**2**/**3** phases, based on PXRD, optical observation and TGA.

structure when the doping level of $L_1$ increases. The solvent weight losses measured by TGA supported the above identification of interpenetrated vs non-interpenetrated phases as shown in Figure 2b. Going from IRMOF-9 to IRMOF-10 structure (with a mixture of both IRMOF-9 and IRMOF-10 phases in the intermediate range), the solvent weight loss of the samples increases from 44% for the IRMOF-9 phase with 4.5% doped $L_1$ to 68% for MOF-**1** with the IRMOF-10 structure. The amounts of the $L_1$ ligand in these crystals were quantified by UV−vis spectroscopy (Table 2). The steric demand of the $L_1$ ligand drives phase transition from interpenetrated to more open, non-interpenetrated structure, showing the importance of ligand size in systematic ligand doping.

**Systematic Doping Studies of $L_2$- and $L_3$-Based MOFs.** Unlike the dinegative $L_1$ ligand, mononegative $L_2$ and neutral $L_3$ ligands do not readily assemble into the $Zn_4O(L)_3$ open framework. Reactions of many kinds of zinc salts with $H_2L_2$ or and $H_2L_3$ in various mixed solvents at 80−100 °C afforded amorphous solids or powdery crystalline samples of unknown structures (Supporting Information). Nonetheless, we successfully doped a small fraction of $L_2$ and $L_3$ into IRMOF-9 or IRMOF-10 frameworks (built from pure BPDC ligand) by taking advantage of matching ligand lengths between BPDC and $L_2/L_3$. This mix-and-match strategy can incorporate sterically demanding phosphors into the IRMOF structure and retain the intrinsic porosity at the same time.

Yellow-red crystals with thin plate or feather-like morphologies were obtained after reacting $H_2L_2/H_2L_3$, $H_2$BPDC, and $Zn(NO_3)_2{\cdot}6H_2O$ in DMF at 90−100 °C for 1−2 days. PXRD analyses indicated the formation of doped IRMOF frameworks with certain $Zn(NO_3)_2/H_2L/H_2$BPDC molar ratios. Observations under polarized light and TGA analyses showed that the interpenetrated IRMOF-9 phase was obtained in both $L_2$- and $L_3$-doped systems. These phases show solvent weight loss ranging from 43 to 47% (Supporting Information). The amounts of $L_2$ and $L_3$ ligands in the crystals were quantified by UV−vis spectroscopy. As listed in Table 2, approximately 8% $L_2$ and 6% $L_3$ can be doped into the IRMOF-9 framework.

When the $L_2/H_2$BPDC or $L_3/H_2$BPDC ratio increases, a new phase emerges. PXRD patterns of the new phases resulting from $L_2$ and $L_3$ doping are very similar (Figure 4), whereas single crystal X-ray crystallography established the phases to be $Zn_2(L_2)(BPDC)_{1.5}{\cdot}(DMF)_2{\cdot}(H_2O)_7$ (MOF-**2**) and $Zn_2(L_3)_{0.5}(BPDC)_2{\cdot}(DMF)_9{\cdot}(H_2O)_8$ (MOF-**3**), respectively. Structure of MOF-**3** has been reported by us earlier.[65] Both phases crystallize in the $C222_1$ space group. In both structures,


dx.doi.org/10.1021/ic402015q | Inorg. Chem. 2014, 53, 1331−1338

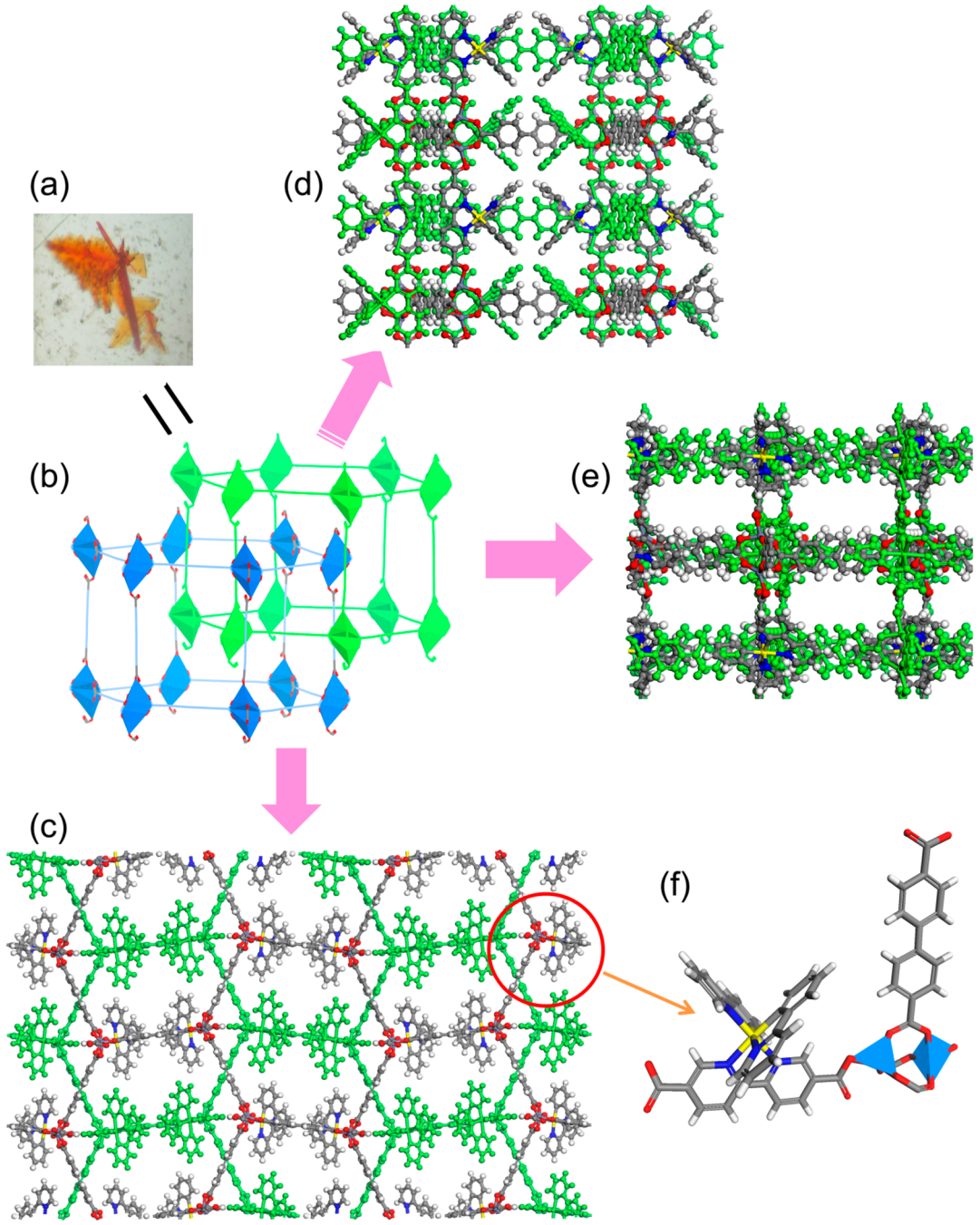


**Figure 3.** (a) A photo of MOF-**2** crystals. (b) A simplified connectivity model showing the interpentrated nets in bnn topology of MOF-**2**. (c) A ball-stick model showing the crystal structure of MOF-**2** viewed along the [001] direction. (d) A ball-stick model showing the crystal structure of MOF-**2** viewed along the [010] direction. (e) A ball-stick model showing the crystal structure of MOF-**2** viewed along the [100] direction. (f) Ball-and-stick and polyhedra presentation of asymmetric unit of MOF-**2**.

triblade paddle wheel $[Zn_2(CO_2)_3]$ SBUs were linked by ditopic BPDC or $\mathbf{L}_2/\mathbf{L}_3$ ligands to form 3D frameworks (Figure 3f). In the asymmetric unit, 5/2 of the dicarboxylate ligands (BPDC and $\mathbf{L}_2/\mathbf{L}_3$) and one $Zn_2$ triblade paddle wheel cluster are present. In the equatorial positions of the triblade paddle wheel, three bidentate carboxylate groups of 1/2 occupancies bridge the two Zn atoms in the SBU. These SBUs are linked by the ligand struts to form a two-dimensional (2D) graphene net. In the axial positions of the Zn paddle wheel, a dicarboxylate ligand with two monodentate carboxylate groups coordinated to the two Zn atoms, further linking the 2D nets to 3D frameworks of 5-connected bnn topology (Figure 2b). As a result of the elongated BPDC and $\mathbf{L}_2/\mathbf{L}_3$ ligands, 2-fold interpenetrated structures were adopted by both MOFs (Figure 2b). There are three crystallographically distinct dicarboxylate ligand positions, among which two of them are in the equatorial positions with respect to the $Zn_2$ paddle wheel, and one of them is in the axial position. Except for one of the equatorial dicarboxylate ligand positions, which is exclusively occupied by BPDC, the other two positions are mixedly occupied by BPDC and $\mathbf{L}_2/\mathbf{L}_3$. The $\mathbf{L}_2/\mathbf{L}_3$ ligands in the equatorial positions can further disorder over two orientations resulting from a 180° rotation along the C−C bond between the carboxylates and aromatic rings. Because of weak diffraction and limited data set


dx.doi.org/10.1021/ic402015q | *Inorg. Chem.* 2014, 53, 1331−1338

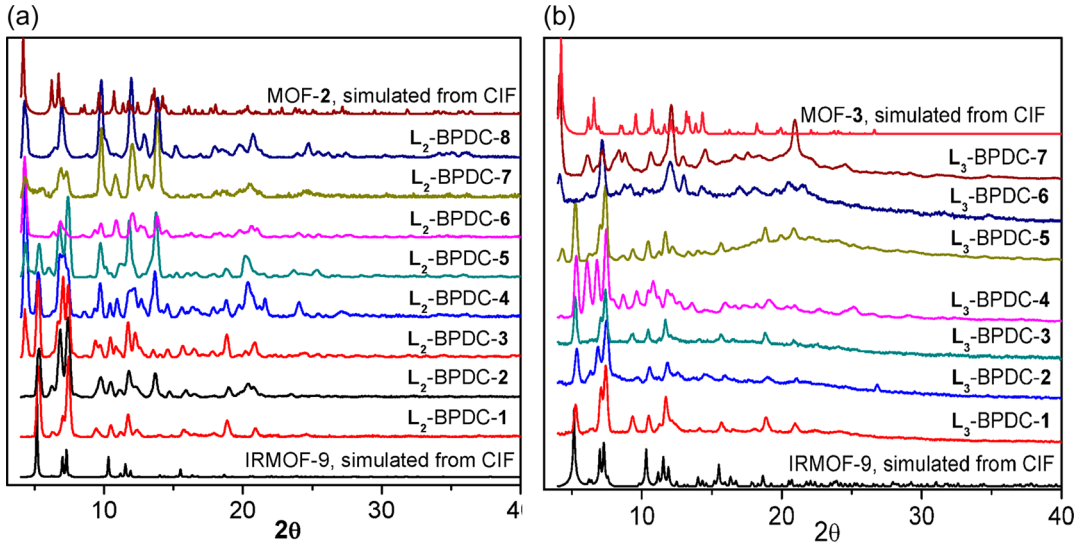


**Figure 4.** Powder X-ray diffractions of (a) $L_2$-doped BPDC-Zn system (b) $L_3$-doped BPDC-Zn system. The preparation condition/$L_{2/3}$ content/identified phases of all the samples in (a) and (b) were listed in Table 2.

**Table 3. Rhodamine 6G Dye Uptake in the Doped MOFs**

| sample number* | structure and phase | doping level L/(L + BPDC) (%) | void space percentage calculated by Platon (%) | dye uptake as wt % of the framework (%) | effective dye concentration inside the MOF channels (mM) |
|---|---|---|---|---|---|
| $L_1$-BPDC-5 | IRMOF-10 (MOF-1) | 100 | 79 | 11.3 | 252 |
| $L_1$-BPDC-1 | IRMOF-9 | 4.5 | 67 | 9.8 | 213 |
| $L_2$-BPDC-6 | MOF-2 | 40 | 45 | 1.7 | 63 |
| $L_2$-BPDC-1 | IRMOF-9 | 6 | 65 | 11.1 | 254 |
| $L_3$-BPDC-6 | MOF-3 | 20 | 60 | 6.1 | 126 |
| $L_3$-BPDC-3 | IRMOF-9 | 6 | 65 | 10.3 | 231 |

*The preparation condition/L content/identified phases of all the samples in (a) and (b) were listed in Table 2.

qualities, the degree of occupancies of the phosphor-based ligands in these mixedly occupied equatorial and axial positions cannot be reliably deduced from single crystal X-ray diffraction studies. The Ir/Ru-complex contents in both of the MOFs were obtained by UV−vis spectroscopy as shown in Table 2. The single crystal structure was then refined against the X-ray data by fixing the $L_2/L_3$ to BPDC ratio in the mixed ligands positions, based on the result from spectroscopic analysis. In MOF-2, the determined framework formula was $Zn_2(L_2)(BPDC)_{1.5}$, equating to 1/2 $L_2$ vs 1/2 BPDC ligands in the mixed ligand positions; in MOF-3, the determined framework formula turned out to be $Zn_2(L_3)_{0.5}(BPDC)_2$, equating to 1/3 $L_3$ vs 2/3 BPDC ligands in the mixed ligand positions. Solvent contents in the channels were determined by a combination of TGA and $^1$H NMR (Supporting Information).

**Assessing the Open Channels in Phosphor Ligand-Doped MOFs.** From the crystal structures, all of the MOFs 1−3 contain internal porosities. Nitrogen adsorption did not afford permanent porosities for these MOFs (Supporting Information), presumably due to severe framework distortion upon the removal of solvent molecules.[16,17,66−69] Instead, we resorted to a dye uptake assay recently developed in our lab to assess and quantify the intrinsic porosity of the MOFs 1−3.[16,17] This method does not require removing solvent molecules from the MOF channel in vacuum and thus preserves the intrinsic porosity of the MOFs. By soaking of the MOFs in a solution of 42 mM rhodamine 6G dye in ethanol for 16 h, significant fractions of the rhodamine 6G were absorbed into the internal channels of the MOFs, by taking advantage of the hydrophobic nature of the MOFs channels. The dye solution was then decanted and the MOFs were quickly washed with water three times to remove dye molecules adsorbed on the external surfaces of the crystals. The dye-loaded MOFs were then digested with disodium ethylenediaminetetraacetic acid ($Na_2EDTA$) and NaOH. The amounts of released rhodamine 6G were quantified by UV−visible spectroscopy after acidifying the solution to pH 1.1. As shown in Table 3, the MOFs exhibit high dye uptake capacities ranging from 1.7 wt % to 11.3 wt % of the framework. The amounts of uptaken dye depend upon the open channels and correspond to an effective dye concentration of 63−254 mM in the MOF channels (equivalent to 1.5−6.0 times of the original dye concentration in the EtOH solution). These results unambiguously prove the accessibility of the open channels of the MOFs.

## DISCUSSION

The $L_1$ ligand can be doped into the IRMOF-9/-10 structures (with BPDC as the ligand) at 0−100% doping levels, thanks to the matching length and charge between $L_1$ and BPDC. However, the steric bulk of $L_1$ ligand induces a phase transition from the interpenetrated IRMOF-9 structure to the non-interpenetrated IRMOF-10 structure, highlighting the important role of the ligand size effect on ligand doping in MOFs.

Within the determined formulas for MOF-2 and MOF-3, both structures obtain neutral frameworks. We propose that the


dx.doi.org/10.1021/ic402015q | Inorg. Chem. 2014, 53, 1331−1338

formation of a neutral framework provides the driving force toward the formation of the new phases of the bnn topology.

By doping the Ir/Ru phosphor-based ligands $\mathbf{L_1}$–$\mathbf{L_3}$ into the BPDC-Zn system, we have successfully obtained three series of doped MOFs as a result of different charges of the doping ligand. The $\mathbf{L_2}$ and $\mathbf{L_3}$ ligands, carrying −1 and 0 charges, respectively, can only be doped into the IRMOF-9 structure to certain doping levels, after which the formation of a new phase with neutral framework of the bnn topology wins over the positively charged, doped IRMOF-9 structure. The dinegative $\mathbf{L_1}$ ligand, on the other hand, forms solid solutions with $H_2$BPDC in IRMOF-9/-10 structure in the whole range of $H_2\mathbf{L_1}/H_2$BPDC ratio, as a result of neutral framework structures of $\mathbf{L_1}$-doped IRMOF-9/-10. It is also worth noting that we failed to obtain a neutral framework of the bnn topology with the $\mathbf{L_1}$ ligand in any $\mathbf{L_1}$/BPDC ratio. The charge balance in the framework thus dictates the degree of doping and the formation of different phases for the doped structures.

Our observations are consistent with the predominance of neutral framework structures of MOFs. The most commonly employed SBUs such as $[Zn_4(\mu_4\text{-O})(\text{carboxylate})_6]$, $[Cu_2(\text{carboxylate})_4(\text{sol})_2]$, and $[Zr_6(\mu_3\text{-O})_4(\mu_3\text{-OH})_4\text{-}(\text{carboxylate})_{12}]$ are all charge-balanced, which form neutral frameworks if no additional charges are present on the ligands.[6,26,70] Even for the $[M(III)_3(\mu_3\text{-O})\text{-}(\text{carboxylate})_6(\text{sol})_3]^+$ SBU in the MIL-101 structure (M = $Fe^{3+}$, $Cr^{3+}$), an anion such as $Cl^-$ typically coordinates to the SBU to lead to a neutral framework.[71] Although cation-templated MOF structures have been reported,[72−74] their appearance frequency is much lower that than that observed for zeolites or metal phosphates.[75,76] Cationic frameworks with charge-balancing anions in the MOF channels have been reported even less frequently.[77−79] The lower tendency for MOFs to adopt an anionic framework in comparison to zeolites and phosphates is likely a result of larger channel sizes of MOFs and more hydrophobic nature of MOF channels. The larger MOF channel size attenuates Coulombic interactions between the cation in the cavity and the anionic framework as a result of larger averaged distance between the two. In a channel larger than 1 nm, the cation can be solvated, which further reduces the Coulombic interaction through a screening effect. Hydrophobic nature of MOF channels also presents an energetic penalty for the framework−ion interactions, further disfavoring the formation of charged MOF frameworks.

## CONCLUSION

We have performed systematic studies on doping three sterically demanding Ir/Ru phosphor-based dicarboxylate ligands of varying charges into the known IRMOF-9/-10 structures. The maximum doping levels of these ligands depend on the charge of the ligands. All of the doped systems exhibit a strong tendency of adopting neutral framework structures. This observation is consistent with the general trend of reported MOF structures in the literature: neutral frameworks appear in a much higher frequency than charged ones. Bulky ligands in the doped MOFs also exert strong steric effects to steer the formation of more spacious, non-interpenetrated structures. These findings indicate important roles of steric demand and charge balance on ligand doping in MOFs, which has been well-established in metal ion doping in traditional inorganic materials.

## ASSOCIATED CONTENT

### Supporting Information

Crystallographic information files; procedures for ligand synthesis; synthesis and characterization procedures of doped MOF series (NMR, TGA, PXRD); X-ray determination; crystal data and structure refinements for MOFs **1**−**3**; spacing-filling models; $N_2$ adsorption isotherms. This material is available free of charge via the Internet at http://pubs.acs.org.

## AUTHOR INFORMATION

### Corresponding Author

*E-mail: wenbinlin@uchicago.edu.

### Notes

The authors declare no competing financial interest.

## ACKNOWLEDGMENTS

We acknowledge NSF-DMR for funding support. C.W. acknowledges UNC Department of Chemistry for a Venable Award.

## REFERENCES

(1) Kitagawa, S.; Kitaura, R.; Noro, S. *Angew. Chem., Int. Ed. Engl.* **2004**, *43*, 2334.
(2) Ferey, G.; Mellot-Draznieks, C.; Serre, C.; Millange, F. *Acc. Chem. Res.* **2005**, *38*, 217.
(3) Long, J. R.; Yaghi, O. M. *Chem. Soc. Rev.* **2009**, *38*, 1213.
(4) Farha, O. K.; Hupp, J. T. *Acc. Chem. Res.* **2010**, *43*, 1166.
(5) Tanabe, K. K.; Cohen, S. M. *Chem. Soc. Rev.* **2011**, *40*, 498.
(6) Eddaoudi, M.; Kim, J.; Rosi, N.; Vodak, D.; Wachter, J.; O'Keeffe, M.; Yaghi, O. M. *Science* **2002**, *295*, 469.
(7) Zhao, D.; Yuan, D. Q.; Zhou, H. C. *Energy Environ. Sci.* **2008**, *1*, 222.
(8) Murray, L. J.; Dinca, M.; Long, J. R. *Chem. Soc. Rev.* **2009**, *38*, 1294.
(9) Allendorf, M. D.; Houk, R. J.; Andruszkiewicz, L.; Talin, A. A.; Pikarsky, J.; Choudhury, A.; Gall, K. A.; Hesketh, P. J. *J. Am. Chem. Soc.* **2008**, *130*, 14404.
(10) Lan, A.; Li, K.; Wu, H.; Olson, D. H.; Emge, T. J.; Ki, W.; Hong, M.; Li, J. *Angew. Chem., Int. Ed. Engl.* **2009**, *48*, 2334.
(11) Xie, Z.; Ma, L.; deKrafft, K. E.; Jin, A.; Lin, W. *J. Am. Chem. Soc.* **2009**, *132*, 922.
(12) Lu, G.; Hupp, J. T. *J. Am. Chem. Soc.* **2010**, *132*, 7832.
(13) Cho, S. H.; Ma, B.; Nguyen, S. T.; Hupp, J. T.; Albrecht-Schmitt, T. E. *Chem. Commun.* **2006**, 2563.
(14) Ma, L.; Abney, C.; Lin, W. *Chem. Soc. Rev.* **2009**, *38*, 1248.
(15) Banerjee, M.; Das, S.; Yoon, M.; Choi, H. J.; Hyun, M. H.; Park, S. M.; Seo, G.; Kim, K. *J. Am. Chem. Soc.* **2009**, *131*, 7524.
(16) Ma, L.; Falkowski, J. M.; Abney, C.; Lin, W. *Nat. Chem.* **2010**, *2*, 838.
(17) Song, F.; Wang, C.; Falkowski, J. M.; Ma, L.; Lin, W. *J. Am. Chem. Soc.* **2010**, *132*, 15390.
(18) deKrafft, K. E.; Xie, Z.; Cao, G.; Tran, S.; Ma, L.; Zhou, O. Z.; Lin, W. *Angew. Chem., Int. Ed. Engl.* **2009**, *48*, 9901.
(19) Della Rocca, J.; Lin, W. *Eur. J. Inorg. Chem.* **2010**, 3725.
(20) Liu, D.; Huxford, R. C.; Lin, W. *Angew. Chem., Int. Ed. Engl.* **2011**, *50*, 3696.
(21) Horcajada, P.; Chalati, T.; Serre, C.; Gillet, B.; Sebrie, C.; Baati, T.; Eubank, J. F.; Heurtaux, D.; Clayette, P.; Kreuz, C.; Chang, J. S.; Hwang, Y. K.; Marsaud, V.; Bories, P. N.; Cynober, L.; Gil, S.; Ferey, G.; Couvreur, P.; Gref, R. *Nat. Mater.* **2009**, *9*, 172.
(22) Rieter, W. J.; Pott, K. M.; Taylor, K. M.; Lin, W. *J. Am. Chem. Soc.* **2008**, *130*, 11584.
(23) Lin, W.; Rieter, W. J.; Taylor, K. M. *Angew. Chem., Int. Ed. Engl.* **2009**, *48*, 650.
(24) Ma, L.; Lee, J. Y.; Li, J.; Lin, W. *Inorg. Chem.* **2008**, *47*, 3955.
(25) Ma, L.; Lin, W. *J. Am. Chem. Soc.* **2008**, *130*, 13834.

(26) Cavka, J. H.; Jakobsen, S.; Olsbye, U.; Guillou, N.; Lamberti, C.; Bordiga, S.; Lillerud, K. P. *J. Am. Chem. Soc.* **2008**, *130*, 13850.
(27) Li, Q.; Zhang, W.; Miljanic, O. S.; Sue, C. H.; Zhao, Y. L.; Liu, L.; Knobler, C. B.; Stoddart, J. F.; Yaghi, O. M. *Science* **2009**, *325*, 855.
(28) Lin, X.; Telepeni, I.; Blake, A. J.; Dailly, A.; Brown, C. M.; Simmons, J. M.; Zoppi, M.; Walker, G. S.; Thomas, K. M.; Mays, T. J.; Hubberstey, P.; Champness, N. R.; Schroder, M. *J. Am. Chem. Soc.* **2009**, *131*, 2159.
(29) Guillerm, V.; Gross, S.; Serre, C.; Devic, T.; Bauer, M.; Ferey, G. *Chem. Commun.* **2010**, *46*, 767.
(30) Lin, W.; Evans, O. R.; Xiong, R. G.; Wang, Z. *J. Am. Chem. Soc.* **1998**, *120*, 13272.
(31) Evans, O. R.; Xiong, R. G.; Wang, Z.; Wong, G. K.; Lin, W. *Angew. Chem., Int. Ed. Engl.* **1999**, *38*, 536.
(32) Evans, O. R.; Lin, W. *Chem. Mater.* **2001**, *13*, 3009.
(33) Evans, O. R.; Lin, W. *Chem. Mater.* **2001**, *13*, 2705.
(34) Wu, C. D.; Hu, A.; Zhang, L.; Lin, W. *J. Am. Chem. Soc.* **2005**, *127*, 8940.
(35) Banerjee, M.; Das, S.; Yoon, M.; Choi, H. J.; Hyun, M. H.; Park, S. M.; Seo, G.; Kim, K. *J. Am. Chem. Soc.* **2009**, *131*, 7524.
(36) Tanabe, K. K.; Cohen, S. M. *Angew. Chem., Int. Ed. Engl.* **2009**, *48*, 7424.
(37) Taylor-Pashow, K. M. L.; Rocca, J. D.; Xie, Z.; Tran, S.; Lin, W. *J. Am. Chem. Soc.* **2009**, *131*, 14261.
(38) Kleist, W.; Jutz, F.; Maciejewski, M.; Baiker, A. *Eur. J. Inorg. Chem.* **2009**, 3552.
(39) Deng, H.; Doonan, C. J.; Furukawa, H.; Ferreira, R. B.; Towne, J.; Knobler, C. B.; Wang, B.; Yaghi, O. M. *Science* **2010**, *327*, 846.
(40) Marx, S.; Kleist, W.; Huang, J.; Maciejewski, M.; Baiker, A. *Dalton Trans.* **2010**, *39*, 3795.
(41) Kent, C. A.; Mehl, B. P.; Ma, L.; Papanikolas, J. M.; Meyer, T. J.; Lin, W. *J. Am. Chem. Soc.* **2010**, *132*, 12767.
(42) Fukushima, T.; Horike, S.; Inubushi, Y.; Nakagawa, K.; Kubota, Y.; Takata, M.; Kitagawa, S. *Angew. Chem., Int. Ed. Engl.* **2010**, *49*, 4820.
(43) Wang, C.; Xie, Z.; deKrafft, K. E.; Lin, W. *J. Am. Chem. Soc.* **2011**, *133*, 13445.
(44) Burrows, A. D. *CrystEngComm* **2011**, *13*, 3623.
(45) Burrows, A. D.; Fisher, L. C.; Richardson, C.; Rigby, S. P. *Chem. Commun.* **2011**, *47*, 3380.
(46) Barrett, S. M.; Wang, C.; Lin, W. *J. Mater. Chem.* **2012**, *22*, 10329.
(47) Caskey, S. R.; Wong-Foy, A. G.; Matzger, A. J. *J. Am. Chem. Soc.* **2008**, *130*, 10870.
(48) Botas, J. A.; Calleja, G.; Sanchez-Sanchez, M.; Orcajo, M. G. *Langmuir* **2010**, *26*, 5300.
(49) Li, H. H.; Shi, W.; Zhao, K. N.; Li, H.; Bing, Y. M.; Cheng, P. *Inorg. Chem.* **2012**, *51*, 9200.
(50) Falcaro, P.; Furukawa, S. *Angew. Chem., Int. Ed. Engl.* **2012**, *51*, 8431.
(51) Rao, X. T.; Huang, Q.; Yang, X. L.; Cui, Y. J.; Yang, Y.; Wu, C. D.; Chen, B. L.; Qian, G. D. *J. Mater. Chem.* **2012**, *22*, 3210.
(52) Adachi, S. *Properties of Group-IV, III-V and II-VI Semiconductors*; John Wiley & Sons: New York, 2005.
(53) Yu, P. Y.; Cardona, M. In *Fundamentals of Semiconductors: Physics and Materials Properties*, 4th ed.; Springer: New York, 2010; p 1.
(54) Caspar, J. V.; Kober, E. M.; Sullivan, B. P.; Meyer, T. J. *J. Am. Chem. Soc.* **1982**, *104*, 630.
(55) Durham, B.; Caspar, J. V.; Nagle, J. K.; Meyer, T. J. *J. Am. Chem. Soc.* **1982**, *104*, 4803.
(56) Gust, D.; Moore, T. A.; Moore, A. L. *Acc. Chem. Res.* **2009**, *42*, 1890.
(57) Baldo, M. A.; Lamansky, S.; Burrows, P. E.; Thompson, M. E.; Forrest, S. R. *Appl. Phys. Lett.* **1999**, *75*, 4.
(58) Lamansky, S.; Djurovich, P.; Murphy, D.; Abdel-Razzaq, F.; Lee, H. E.; Adachi, C.; Burrows, P. E.; Forrest, S. R.; Thompson, M. E. *J. Am. Chem. Soc.* **2001**, *123*, 4304.
(59) Tamayo, A. B.; Alleyne, B. D.; Djurovich, P. I.; Lamansky, S.; Tsyba, I.; Ho, N. N.; Bau, R.; Thompson, M. E. *J. Am. Chem. Soc.* **2003**, *125*, 7377.
(60) Bock, C. R.; Meyer, T. J.; Whitten, D. G. *J. Am. Chem. Soc.* **1974**, *96*, 4710.
(61) Kent, C. A.; Liu, D.; Meyer, T. J.; Lin, W. *J. Am. Chem. Soc.* **2012**, *134*, 3991.
(62) Ischay, M. A.; Anzovino, M. E.; Du, J.; Yoon, T. P. *J. Am. Chem. Soc.* **2008**, *130*, 12886.
(63) Narayanam, J. M.; Tucker, J. W.; Stephenson, C. R. *J. Am. Chem. Soc.* **2009**, *131*, 8756.
(64) Condie, A. G.; Gonzalez-Gomez, J. C.; Stephenson, C. R. *J. Am. Chem. Soc.* **2010**, *132*, 1464.
(65) Wang, C.; Lin, W. *J. Am. Chem. Soc.* **2011**, *133*, 4232.
(66) Ghoufi, A.; Maurin, G. *J. Phys. Chem. C* **2010**, *114*, 6496.
(67) Llewellyn, P. L.; Maurin, G.; Devic, T.; Loera-Serna, S.; Rosenbach, N.; Serre, C.; Bourrelly, S.; Horcajada, P.; Filinchuk, Y.; Ferey, G. *J. Am. Chem. Soc.* **2008**, *130*, 12808.
(68) Neimark, A. V.; Coudert, F. X.; Boutin, A.; Fuchs, A. H. *J. Phys. Chem. Lett.* **2010**, *1*, 445.
(69) Serre, C.; Millange, F.; Thouvenot, C.; Nogues, M.; Marsolier, G.; Louer, D.; Ferey, G. *J. Am. Chem. Soc.* **2002**, *124*, 13519.
(70) Ma, L.; Lin, W. *J. Am. Chem. Soc.* **2008**, *130*, 13834.
(71) Latroche, M.; Surble, S.; Serre, C.; Mellot-Draznieks, C.; Llewellyn, P. L.; Lee, J. H.; Chang, J. S.; Jhung, S. H.; Ferey, G. *Angew. Chem., Int. Ed. Engl.* **2006**, *45*, 8227.
(72) Yang, S.; Lin, X.; Blake, A. J.; Walker, G. S.; Hubberstey, P.; Champness, N. R.; Schröder, M. *Nat. Chem.* **2009**, *1*, 487.
(73) An, J.; Geib, S. J.; Rosi, N. L. *J. Am. Chem. Soc.* **2009**, *131*, 8376.
(74) Dinca, M.; Long, J. R. *J. Am. Chem. Soc.* **2007**, *129*, 11172.
(75) Cheetham, A. K.; Ferey, G.; Loiseau, T. *Angew. Chem., Int. Ed. Engl.* **1999**, *38*, 3268.
(76) Jiang, J. X.; Yu, J. H.; Corma, A. *Angew. Chem., Int. Ed. Engl.* **2010**, *49*, 3120.
(77) Zheng, S. T.; Bu, J. J.; Wu, T.; Chou, C. T.; Feng, P. Y.; Bu, X. H. *Angew. Chem., Int. Ed. Engl.* **2011**, *50*, 8858.
(78) Wang, C.; deKrafft, K. E.; Lin, W. *J. Am. Chem. Soc.* **2012**, *134*, 7211.
(79) Wang, C.; Wang, J.-L.; Lin, W. *J. Am. Chem. Soc.* **2012**, *134*, 19895.